Spermidine and Spermine Catalyze the Formation of Nanostructured Titanium Oxide

Kathryn E. Cole and Ann M. Valentine*

Department of Chemistry, Yale University, New Haven, Connecticut 06511

Received December 22, 2006; Revised Manuscript Received March 1, 2007

Naturally occurring polyamines putrescine, cadaverine, spermidine, and spermine are analogues of the species-specific long-chain polyamines found in diatoms. Scanning electron microscopy and energy-dispersive spectroscopy show that the reactions of a soluble Ti(IV) precursor with spermidine and spermine, but not putrescine or cadaverine, produce nanostructured irregular polyhedra of titanium oxide. At 25 °C, the average size of the particles formed with spermidine is 400 ± 150 nm, and with spermine, 140 ± 50 nm. Although the particles are X-ray amorphous at room temperature, annealing studies reveal that the particles adopt crystallinity at higher temperatures characteristic of anatase (TiO_2). The major portion of the biopolyamines is not coprecipitated with the solid but is left in solution. Kinetic measurements reveal an initial fast step followed by two slower phases of reaction. At 25 °C, k_{1obs} and k_{2obs} for the reaction with spermidine are 5×10^{-3} s^{-1} and 3.6×10^{-4} s^{-1}, respectively, and for spermine, 4.8×10^{-3} s^{-1} and 4.2×10^{-4} s^{-1}, respectively. Taken together, the data suggest spermidine and spermine are biocatalysts for the precipitation of nanostructured titanium oxide.

Introduction

Polyamines are found in the cells of most living organisms.[1] Although their specific cellular roles are not fully known, natural polyamines (putrescine, cadaverine, spermidine, and spermine, Figure 1) are essential for the proper growth, differentiation, and apoptosis of cells and have been conserved through evolution.[2,3] With pK_a values for the protonated nitrogens above 8,[1] each nitrogen is positively charged at physiological pH, making the molecule overall polycationic.

The biomolecules involved in diatom frustule construction (biosilicification) have been isolated and found to include polyamine moieties.[4−6] Cationic polypeptides isolated from diatoms, called silaffins, often contain long-chain polyamine modifications to lysine (Figure 1). These polyamines are anchored to the peptide through putrescine, or a putrescine derivative, and are some of the longest found in nature, with up to 20 repeating propylamine units.[5,7] The isolated long-chain polyamines vary among species and may be responsible for the differences observed in frustule morphologies.

The isolated diatom polyamines induce the precipitation of silica from a soluble silicic acid precursor solution in vitro.[5] Poly(allylamine), a synthetic mimic of the isolated polyamines, also precipitates nanostructured silica.[5,8,9] Recent work investigates the silica nanostructures formed with naturally occurring polyamines derived from putrescine.[10,11] Mechanisms for silica precipitation with polyamines have been suggested.[10,12−14] A recent review describes the general mechanisms involved in biomineralization.[15]

Compared with that of silica, the biological role of titanium is not well understood. Although titanium is prevalent in the earth's crust and can be found in seawater,[16] the biologically related occurrence of mineralized titanium is rare, although a few examples are known.[17−19] The hornet *Vespa orientalis* incorporates mineral grains in each comb of its nest.[17] The uniformly sized grains are largely composed of iron, titanium, and oxygen, suggesting they may be grains of ilmenite ($FeTiO_3$).[18] In another example, needles composed of titanium and oxygen were found embedded in the test of the foraminiferan *Bathysiphon argenteus*.[19] In each of the previous two examples, it is unclear whether the organism produces the titanium mineral or collects it from the environment. Titanium mineralization has also been reported in humans, notably in leukocytes and osteosarcomas. In human blood serum, titanium concentrations average about 2 μM.[20] More than a 10-fold higher concentration

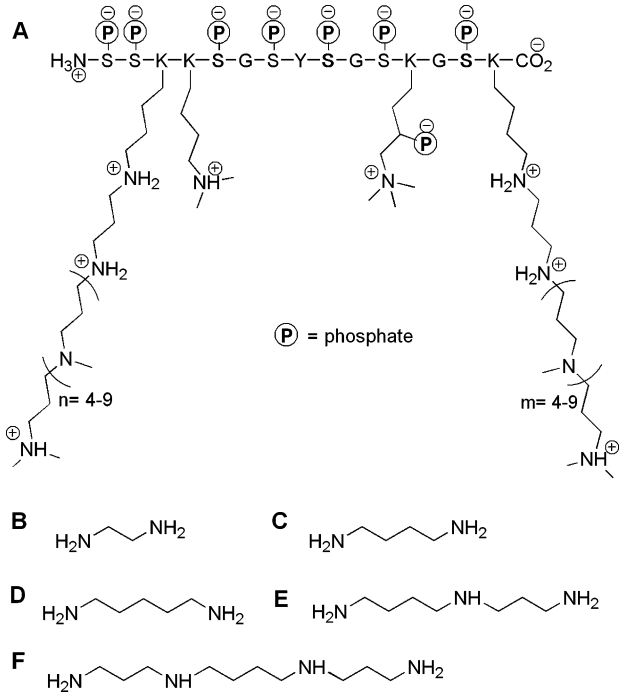

Figure 1. Polyamines of interest: (A) chemical structure of a polyamine-modified silaffin (adapted from ref 9), (B) ethylenediamine, (C) putrescine, (D) cadaverine, (E) spermidine, and (F) spermine. Protonated amines are shown for the silaffin but not for the other polyamines.

* Author to whom correspondence should be addressed. E-mail: ann.valentine@yale.edu.

10.1021/bm061221l CCC: $37.00
Published on Web 04/20/2007

occurs in leukocytes from some patients with Hodgkin's lymphoma or leukemia, as compared to normal subjects or subjects having other disorders.[21,22] Finally, an attempt to probe the distribution of titanium in untreated osteoblastic osteosarcoma cells revealed mineral clusters near the nucleus that contained very high concentrations of titanium.[23]

Diatoms may also incorporate titanium into their frustules.[24−27] In addition to silica, the R5 peptide[28,29] (H_2N-SSKKSGSYSG-SKGSKRRIL-COOH), derived from a repeat unit of a silaffin from the diatom *Cylindrotheca fusiformis*, and analogous recombinant silaffin peptides[30] precipitate micro- and nanostructured titanium dioxide. Poly(allylamine), a synthetic mimic of the long-chain polyamines found in diatoms, precipitates titanium phosphate in vitro.[28] This work investigates the ability of spermidine, spermine, and related amines to precipitate nanostructured mineralized titanium in vitro. Given that previous work demonstrated that the R5 peptide alone induced TiO_2[29] and the very long chain polyamine poly(allylamine) induced TiP_2O_7[28] from a soluble titanium precursor, this work studies whether shorter biopolyamines also have the ability to mineralize titanium. These polyamines serve as complementary models for the silaffin-attached polyamines in diatoms, and in view of their prominent role in many biological processes, the results may also be relevant to other examples of biological titanium mineralization.

The precipitated bulk solids are characterized by using scanning electron microscopy, energy-dispersive spectroscopy, and powder X-ray diffraction. The effects of temperature and pH on the size and morphology of the particles are studied. Infrared spectroscopy and nuclear magnetic resonance are used to monitor the polyamine biomolecules before and after reaction to determine whether they are coprecipitated with the solid. The temperature-dependent kinetics of the mineralization reactions are studied by using a spectrophotometric assay to measure rates of reaction and calculate the corresponding enthalpic and entropic parameters. Finally, a possible mechanism of reaction is proposed.

Materials and Methods

Materials. All aqueous stocks were prepared with Nanopure-quality water (18.2 MΩ·cm resistivity). Spermidine (SPDN, CAS 124-20-9, 99%), titanium(IV) bis(ammonium lactato) dihydroxide (TiBALDH, CAS 65104-06-5, 50 wt % in water), and 4,5-dihydroxy-1,3-benzenedisulfonic acid disodium salt monohydrate (Tiron, CAS 270573-71-2) were purchased from Aldrich. Spermine (SPN, CAS 71-44-3, 97%) was purchased from Acros Organics. Putrescine dihydrochloride (CAS 333-93-7) and cadaverine dihydrochloride (CAS 1476-39-7) were purchased from Sigma. Ethylenediamine (CAS 107-15-3, 99%) was purchased from Alfa Aesar. All reagents were used without further purification.

Precipitation Reaction. In a typical reaction with either SPDN or SPN (Figure 1), a 60 μL portion of 1 M TiBALDH in water was added after the addition of 773 μL of water to 667 μL of 30 mM polyamine, yielding final concentrations of 40 mM Ti complex and 13.34 mM polyamine. The reactions with SPDN and SPN maintain a 1:1 and 1:0.75 Ti:N molar ratio, respectively. Similar amine equivalents are reported for the precipitation of silica.[10] Precipitation was evident immediately upon the addition of the titanium precursor in both reactions. Reactions in the absence of polyamine show slight precipitation after weeks. For the reactions with phosphate, the water fraction was substituted with phosphate buffer (0.2 M, pH 7.4). Samples were collected by centrifugation and washed with dH_2O typically three times before analysis. Samples were sent to Atlantic Microlabs for C/H/N elemental analysis.

Experiments with putrescine, cadaverine, and ethylenediamine included 30, 45, or 60 mM stock solutions of amine added to 773 μL of water followed by the addition of 60 μL of 1 M TiBALDH, yielding final diamine concentrations of 13.34, 20.01, and 26.68 mM, respectively, and a final titanium complex concentration of 40 mM. Control experiments with added ammonium lactate (0.03−0.3 M final concentrations) incorporated the ammonium lactate into the water fraction to maintain final reagent concentrations. Spectrophotometric analysis (see below) confirms that the concentration of titanium in solution in the absence of polyamine does not change over several hours.

In variable-temperature experiments, all reagents were equilibrated to the specified temperature in a water bath for >10 min prior to mixing. In variable-pH experiments, ∼1 M HCl and NaOH solutions were used to adjust the pH of the solution prior to the addition of TiBALDH. The HCl and NaOH volumes were included in the water fraction to maintain final reagent concentrations. The solutions were allowed to equilibrate for >20 min before measurement of the pH and addition of TiBALDH. The pH was again measured after the TiBALDH was allowed to react for >5 h. The pH values reported are those measured after the addition of TiBALDH. A table comparing the pH values before and after the addition of TiBALDH is provided (Table S1, Supporting Information.)

Scanning Electron Microscopy/Energy-Dispersive Spectroscopy. Scanning electron microscopy (SEM) was performed on an FEI XL-30-ESEM-FEG instrument at 10−15 kV in high-vacuum mode (<8×10^{-6} Torr). Elemental distribution was determined by energy-dispersive spectroscopy (EDS) analysis. A thin carbon sputter coating (6−9 nm thickness) was required for high vacuum. Carbon tape and a colloidal graphite solution (Ted Pella, Inc.) were used to coat the aluminum mount before the addition of sample.

Image Analysis. SEM images were analyzed by use of the software ImageJ (http://rsb.info.nih.gov/ij/).

Powder X-ray Diffraction. Powder X-ray diffraction (XRD) was performed by using a Bruker-AXS D8 Focus diffractometer with Cu radiation at 1.544 29 Å. Samples were scanned over a range of 10.000−80.000° in a $\theta-2\theta$ locked couple scan.

Annealing Studies. After being dried under vacuum overnight to remove excess water, the solid samples were heated in air in an annealing oven (Special Furnace Co. Inc., model GS1714) in a quartz vial to the required temperature. XRD was used to determine the crystallinity of the samples after heating to each temperature.

Infrared Spectroscopy. Solids were dried under vacuum overnight to remove excess water. Solid samples were analyzed as Nujol mulls on a Nicolet 6700 Fourier transform infrared spectrometer. Typical experiments average 32 scans.

Nuclear Magnetic Resonance. Samples containing 10% D_2O were analyzed on a Bruker 500 MHz instrument with water suppression. Methanol (0.8%) was used an as internal reference and calibrated to 3.207 ppm.

Temperature-Dependent Kinetics Studies. The problem of resolubilizing precipitated titanium minerals has been discussed.[28] Instead, to follow the progress of the reaction, the amount of titanium remaining in solution during the precipitation reaction was monitored by using a spectrophotometric analytical assay,[31] with some modification to the method previously reported.[28] Aliquots (100 μL) were taken at various time intervals from the precipitation reaction and centrifuged for 1−2 min at 10 °C. The resultant supernatants were added to solutions containing Tiron (100 μL of 75.25 mM stock) and sodium acetate buffer (800 μL of 1.5 M stock, pH ∼5.3), yielding final volumes of 1 mL. The Tiron immediately complexes the titanium in solution, producing a yellow-colored mixture. The solutions were allowed to equilibrate for approximately 1 h prior to measurement of A_{380nm}. Concentrated solutions were diluted as necessary to bring the absorbance values below 1.2 absorbance units. The values presented in Figures 5, S9, and S10 are the calculated predilution values determined from the diluted A_{380nm} measurements. Control experiments with increased concentrations of Tiron (200 μL of 75.25 mM Tiron, 700 μL of 1.5 M sodium acetate

buffer) show no change in initial absorbance values, confirming there is enough Tiron to completely complex the titanium in solution.

Additional TiBALDH (10 μL of 1 M stock) was added to freshly precipitated nanoparticles to study the possibility of particle surface reactivity. Nanoparticles precipitated from SPDN at 50 °C were pelleted, the supernatant was removed, and the nanoparticles were subsequently washed three times with 1 mL of water. The remaining particles were resuspended in 1.5 mL of water, and 10 μL of 1 M TiBALDH was added to the mixture. The reaction was monitored by using the spectrophotometric assay, as described above.

A single-exponential decay failed to fit the data adequately, so the absorbance values, reflecting the concentration of titanium still in solution at each time, were fit to two processes. This procedure yielded two rate constants, k_{1obs} and k_{2obs}. The values were plotted according to the methods of Eyring to determine $\Delta H^{\ddagger}$ and $\Delta S^{\ddagger}$.[32,33] The values for $\Delta G_{298}^{\ddagger}$ were calculated from the obtained enthalpic and entropic parameters. Two to four trials were performed at each temperature to ensure the reaction was complete and confirm reproducibility. The experiment was performed in the dark and Tiron stock solutions were prepared fresh to avoid oxidation.

Results and Discussion

Precipitation and Bulk Characterization. Spermidine (SPDN) and spermine (SPN) both induce the rapid precipitation of a white solid from the otherwise water-stable precursor titanium-(IV) bis(ammonium lactato) dihydroxide (TiBALDH) at pH ~9 and 25 °C. Analogous reactions with other polyamines (putrescine, cadaverine, and ethylenediamine) do not induce mineralization; slight precipitation is observed only in the reaction with ethylenediamine after at least 12 h. Thus, at least three amine functionalities appear to be required for rapid reaction.

Scanning electron microscopy (SEM) shows that the solids consist of nanosized irregular polyhedra (Figure 2). Image analysis determines that the particles formed with SPDN at 25 °C range in size from 100 to 800 nm, with an average size of 400 ± 150 nm. The particles formed with SPN at 25 °C range in size from 50 to 300 nm, with an average size of 140 ± 50 nm. Similar structures are formed in the precipitation of silica.[10] These structures are much different than those formed with the R5 peptide and poly(allylamine), which form fused and well-defined nano- and microspheres, respectively.[28,29]

Energy-dispersive spectroscopy (EDS) reveals that the bulk solids are largely composed of titanium and oxygen (Figure S1, Supporting Information). A phosphorus peak also appears in the EDS spectrum when the solid is precipitated in the presence of phosphate buffer, although it is much less intense than previously observed in reactions with poly(allylamine).[28] The phosphate peak becomes smaller, relative to the titanium peak, with repeated washing, although it does not disappear completely. Phosphate is not required for precipitation, in contrast to the reaction of TiBALDH with poly(allylamine). These observations are consistent with reported results for the reaction with silica. Precipitation reactions utilizing long-chain polyamines often require phosphate, or other multivalent anions,[8,12] while those with spermidine and spermine proceed without added buffers or salts.[10] An example of a long-chain polyamine having seven nitrogens that precipitates silica in the absence of phosphate has been reported.[34]

Powder X-ray diffraction (XRD) was used to determine whether the bulk solids are crystalline and exhibit a particular mineral form. The solids precipitated with SPDN and SPN are both X-ray amorphous at room temperature. In order to induce crystallinity and identify a mineral form, the solids were

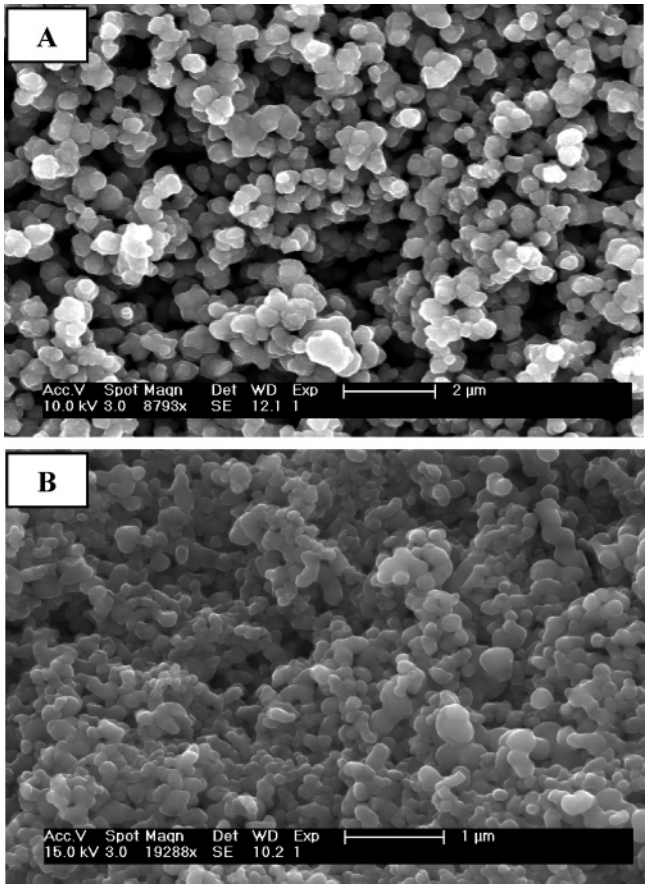

Figure 2. SEM images of titanium oxide solids formed with (A) SPDN and (B) SPN. Scale bars are 2 μm and 1 μm, respectively.

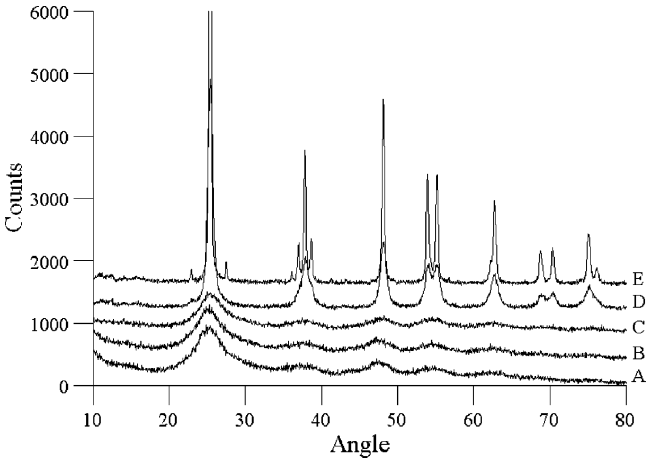

Figure 3. XRD data from solid precipitated with SPDN and annealed to (A) room temperature, (B) 200 °C, (C) 400 °C, (D) 600 °C, and (E) 800 °C.

annealed up to 800 °C. SPDN is largely amorphous through 200 and 400 °C. The solid adopts some crystallinity at 600 °C and strongly diffracts at 800 °C (Figure 3). The diffraction pattern at 800 °C corresponds to that of anatase (Powder Diffraction File database 21-1272) with small amounts of rutile (Powder Diffraction File database 72-1148). The initially off-white solid becomes brown upon annealing to 200 and 400 °C and converts to a white solid upon annealing to 800 °C. The solid precipitated with SPDN in the presence of phosphate has a diffraction pattern, after annealing to 800 °C, that also corresponds to that of anatase (Figure S2, Supporting Information). This result is in contrast to the reaction with poly-

(allylamine), which forms a titanium phosphate solid in the presence of phosphate.[28]

Similar results are observed for the solid precipitated with SPN. After annealing to 800 °C, the solids precipitated in the presence and absence of phosphate both diffract with peaks characteristic of anatase (Figure S3, Supporting Information).

Although some phosphorus, which we have attributed to coprecipitated phosphate, is visible in the EDS data in the presence of phosphate (Figure S2, Supporting Information), no features attributable to a titanium phosphate solid were observed. Thus, while the data do not rule out the formation of a small amount of titanium phosphate when phosphate is present, the bulk of the material is titanium oxide.

Biomolecule Immobilization. The supernatant, after precipitation, is active in precipitating additional titanium oxide, which suggests that a substantial fraction of the biomolecules is still in solution. This observation is in contrast to previous experiments with the R5 peptide and poly(allylamine), in which the (bio)molecules became immobilized in the solid and further precipitation induced by the supernatant was not observed.[28,29] After an initial precipitation with SPDN at room temperature, allowed to react for 12 h to ensure full reaction, the solid was pelleted and the supernatant removed. Precipitation was observed with the addition of more TiBALDH (60 μL of 1 M) to the supernatant. The reaction was slower than the initial precipitation (minutes rather than seconds), although still much faster than in the absence of polyamine. Results similar to those with SPDN are observed for the analogous reactions with SPN.

An increased concentration of released chelating ligands (lactate) may cause slower titanium precipitation in the second reaction. When additional TiBALDH is added to the supernatant, the previously released lactate ligands in solution may favor complexation of the newly added titanium, which prevents it from precipitating. In support of this model, the addition of variable amounts of ammonium lactate (0.03−0.3 M) to the reaction mixture slows precipitation (data not shown). These observations are consistent with the slower precipitations resulting from sequential reactions with SPDN and SPN supernatants.

^{1}H nuclear magnetic resonance (NMR) was used to monitor the polyamines before and after the reactions. A control experiment with SPDN with no TiBALDH shows one set of peaks centered at ca. 2.45 ppm (Figure S4, Supporting Information). These peaks result from the protons on the methylenes next to amines. Another set of peaks is centered at ca. 1.4 ppm, resulting from the protons on the methylenes not flanking amines. These peaks are independent of those associated with the lactate on TiBALDH, which occur between 1.0 and 1.3 ppm and were monitored before and after the reaction.

The spectrum of the supernatant after one precipitation reaction with SPDN shows a resolved set of two peaks centered at ca. 2.75 ppm and another at ca. 1.65 ppm. The spectrum of the supernatant after a second precipitation reveals one very broad peak of low intensity centered at ca. 2.9 ppm. The methylene peaks integrate to only ~60% of the original signal after one precipitation and only ~40% after two precipitations. This result indicates that the amine concentration is decreasing, suggesting some portion may be coprecipitating with the solid. However, the high percentage of biopolyamine remaining in solution is in contrast to the reported results with the R5 peptide and poly(allylamine),[28,29] where both (bio)molecules become immobilized in the solids during precipitation. Similar results are observed for the analogous reactions with SPN.

The increasing broadness and downfield shift of the NMR peaks with both SPDN and SPN can be attributed to small pH changes. As free protons are complexed to the amines, the nearby methylene protons are deshielded, which results in a downfield shift. The increasing peak broadness results from the free proton exchange with the amines. Similar processes may occur with titanium and/or ammonium ions in solution. In addition, the titanium in solution may still be reacting and precipitating during the NMR experiments, which may also influence the broadness of the peaks.

Infrared spectroscopy (IR) and elemental analysis were used to investigate whether the SPDN and SPN biomolecules become immobilized within the solid during precipitation reactions.[28,29,35−37] No amine stretches were observed in Nujol mulls of mineralized titanium oxide (data not shown). The IR spectra of neat commercial SPDN and SPN, however, show extremely broad peaks, indicating polyamine hydration. The IR data from the precipitated solids, therefore, fail to provide evidence for immobilization. Elemental analysis reveals approximately 11.0% carbon, 3.1% hydrogen, and 2.8% nitrogen present in the particles formed with SPDN. Likewise, the particles formed with SPN show 11.7% carbon, 3.3% hydrogen, and 3.1% nitrogen content. These values suggest that a small portion of the biopolyamines is associated with the particles after precipitation.

Effects of Varying Temperature and pH. Variable temperature and pH studies were conducted to observe their effects on the size and morphology of the particles. Mineralizations induced by SPDN at a variety of temperatures show that the nanostructures become smaller when precipitated at higher temperatures (Figure S5, Supporting Information). The broad distribution of sizes (100−900 nm, average size 490 ± 170 nm) (Figure S6) observed at 10 °C changes with increasing temperature to a more narrow size distribution (50−250 nm, average size 150 ± 50 nm) at 80 °C. The rate of reaction is increased overall at higher temperatures (see below), which likely promotes an increase in initial nucleation rate. If more of the titanium precursor is used for sites of nucleation, less is available for particle growth, which results in a greater number of smaller nanosized particles.

Temperature has less of an effect on the morphology of the particles formed during the reaction with SPN. The precipitation with SPN is visibly faster than that with SPDN and so temperature does not so dramatically affect apparent rates of nucleation. The structures appear to maintain size and shape in a temperature range from 5 to 80 °C and resemble the data in Figure 2B. Figure S7 shows that the particles formed with SPN range from approximately 50 to 350 nm regardless of temperature.

The formation of structured solid induced by SPDN is very pH-dependent. At low pH values (~2.5−5.3), no solid is precipitated, even after several days. Near neutral pH, the characteristic irregular polyhedra are formed along with micrometer-sized spheres (Figure 4A). These spheres resemble the titanium phosphate spheres induced by poly(allylamine),[28] but they occur in the absence of phosphate. In the range of pH 8−9 only the characteristic polyhedra are observed, and above pH 9 a decrease in structured solid is noticed, resulting in unstructured material above pH 9.5. With SPN, solid is precipitated in the range of pH ~2.9−12.6. Nanoscale structure is observed between pH 2.5 and 10 (Figure S7, Supporting Information).

The results from the variable-pH experiments are in contrast to those found for poly(allylamine).[28] In the present work the results of variable pH experiments are not clearly explained by SPDN or SPN pK_a values.[1] Instead, precipitation is likely

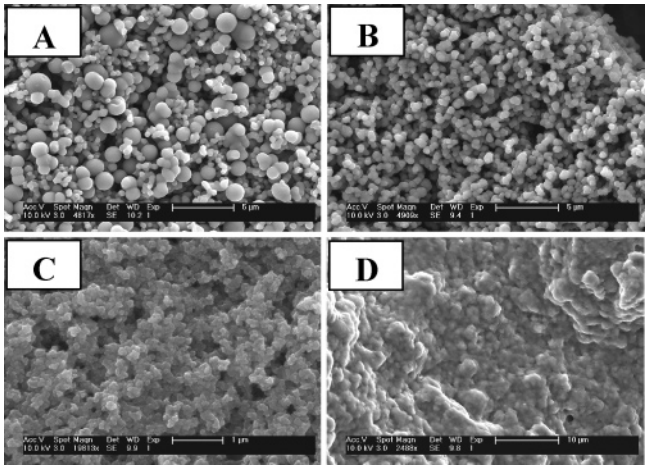

Figure 4. SEM images of SPDN variable-pH experiments at (A) pH 6.7 (scale bar 5 μm), (B) pH 8.9 (scale bar 5 μm), (C) pH 9.3 (scale bar 1 μm), and (D) pH 9.9 (scale bar 10 μm).

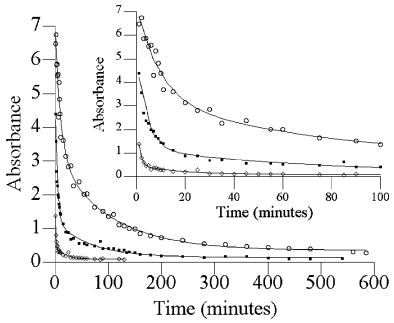

Figure 5. Representative plot showing the amount of Ti^{4+} detected in solution during mineralized induced by SPDN at (○) 10, (■) 20, and (◊) 40 °C.

dominated by the titanium complex speciation in solution. At low pH, titanium is less effective in hydrolyzing water and no precipitation is observed. With increasing pH, on the other hand, titanium more easily hydrolyzes water and precipitates as TiO_2. The TiBALDH complex alone hydrolyzes above pH 12.5.

Kinetics. To gather further evidence regarding the mechanism of precipitation, the kinetics are followed by using a discontinuous spectrophotometric technique to monitor the disappearance of titanium in solution. As expected, precipitation occurs at a faster rate at higher temperatures. Figure 5 shows representative reaction progression at several temperatures; all data for SPDN and SPN are provided in Figures S8 and S9 in the Supporting Information.

In all reactions, at least one step occurs faster than this method can detect. The theoretical starting absorbance for these reactions would be in the range of 10−12 absorbance units; in the absence of polyamine, this level is detected and is constant for hours. The earliest time point achievable by the present method is approximately 1 min, by which time ~50% of the soluble titanium is gone from solution. This period includes particle nucleation. The particles continue to grow, however, and soluble titanium disappearance from solution can be monitored over several hours, depending on temperature.

A single-exponential decay was not sufficient to fit the data. A two-exponential decay fit the data. For SPDN as a precipitation inducer at 25 °C, values of k_{1obs} and k_{2obs} were 5×10^{-3} s^{-1} and 3.6×10^{-4} s^{-1}, respectively, and for SPN they were 4.8×10^{-3} s^{-1} and 4.2×10^{-4} s^{-1}. The observed rates calculated from the plots like those shown in Figure 5 are analyzed in Eyring plots to determine the $\Delta H^{\ddagger}$ and $\Delta S^{\ddagger}$ values

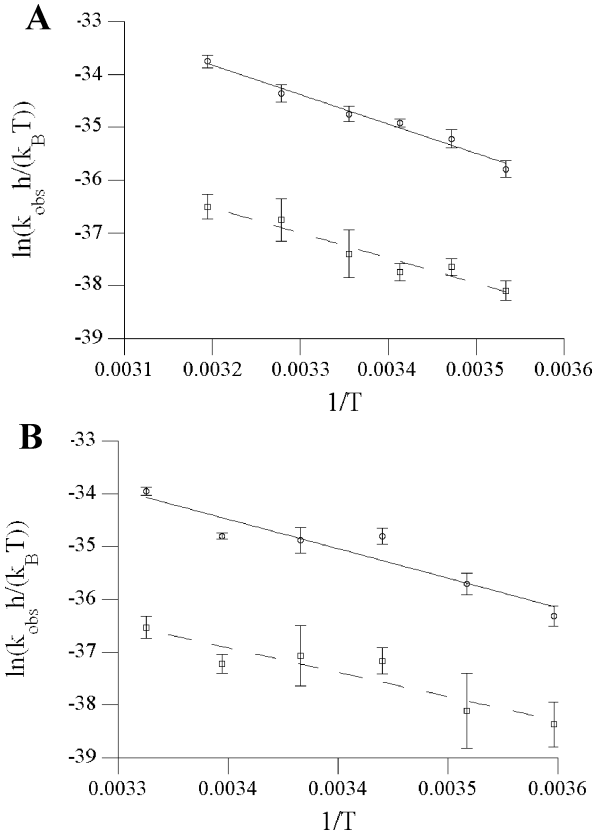

Figure 6. Eyring plots for the reactions with (A) SPDN and (B) SPN: (—) k_{1obs} and (− − −) k_{2obs}.

Table 1. Reaction Parameters Calculated from Eyring Plots for Precipitation Reactions with SPDN and SPN

polyamine		$\Delta H^{\ddagger}$ (kJ/mol)	$\Delta S^{\ddagger}$ (J/mol)	$\Delta G_{298}{}^{\ddagger}$ (kJ/mol)
SPDN	k_{1obs}	46 ± 3	−331 ± 11	145 ± 11
SPDN	k_{2obs}	39 ± 5	−375 ± 17	151 ± 18
SPN	k_{1obs}	58 ± 10	−289 ± 35	144 ± 36
SPN	k_{2obs}	48 ± 10	−343 ± 33	150 ± 34

of the reactions (Figure 6).[32,33] The resulting enthalpic and entropic activation values are provided in Table 1. These are composite values that are calculated by plotting each k_{obs} in the Eyring graphs and contain contributions from all elementary reactions.

The existence of multiple processes is further supported by the decrease in particle size with increasing temperature, particularly for SPDN as discussed above. Increased rates of nucleation at higher temperatures allow for more titanium precursor to be used in the initial nucleation, which results in less particle growth and smaller structures. The nucleation rate induced by SPN may be less sensitive to temperature, with a large number of particles nucleated even at low temperature that grow more slowly.

The enthalpic and entropic parameters for the two phases of reaction, and for the two amines, are similar. With only moderate enthalpic contributions, the free energy barrier for both steps is largely dominated by the highly negative entropic barrier, which is consistent with the formation of a solid. The overall thermodynamic driving force must be very large [ΔG_f (TiO_2, anatase) = −884.5 kJ/mol] so the reaction is favored.

The experiments also support the suggestion that the polyamine biomolecules are not completely coprecipitated with the solid and some fraction is left in solution. Work of Sewell and Wright[29] with the R5 peptide found that only 20% of the initial

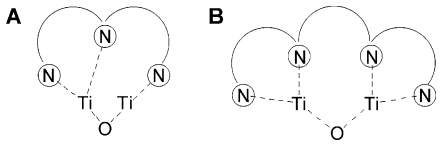

Figure 7. Models of metal complexation with (A) SPDN and (B) SPN.

titanium precursor was precipitated from solution, indicating that the peptide biomolecule became encapsulated in the solid during precipitation. The reactions with SPDN and SPN, however, show mineralization of >92% and >94%, respectively, which is nearly all the titanium precursor that was originally at a Ti:N molar ratio of approximately 1. The high conversions of TiBALDH precursor to TiO_2 product further support that most of the polyamine biomolecules remain in solution after initial precipitation. The increased rate of titanium precipitation in the presence of polyamine, coupled with the phenomenon of the majority of the SPDN and SPN remaining in solution, strongly supports the argument that these biopolyamines are acting as biocatalysts.

Mechanism. Experiments with putrescine, cadaverine, and ethylenediamine provide clues to the mechanism of reaction. Reactions with 30 mM stock solutions (final concentration 13.34 mM) of these diamines did not yield immediate precipitation, in contrast to the analogous reactions with SPDN and SPN, which immediately produced solid. The diamine stock concentrations were increased to 45 mM (final concentration 20.01 mM) and 60 mM (final concentration 26.68 mM) to maintain amine equivalents with SPDN and SPN, respectively. A slight precipitation was observed only with ethylenediamine over days, even at higher concentrations.

The lack of precipitation with putrescine, cadaverine, and ethylenediamine suggests that the number of amine functionalities is important for precipitation. The structures of SPDN and SPN allow for two metal atoms to be complexed by the amines. The models proposed in Figure 7 show that metal complexation might bring two titanium atoms in close proximity, which would induce condensation. The diamines, on the other hand, may complex the titanium atoms by bidentate chelation but fail to bring them into close proximity for condensation, which prevents the titanium from precipitating. Titanium(IV) is known to be labile,[38] so its association with SPDN and SPN does not necessarily result in biopolyamine immobilization.

This model of titanium complexation may help explain the broader pH range observed for precipitation with SPN than SPDN. At low pH, free protons compete with titanium atoms for complexation with the amines. With four amine groups, SPN can more easily complex and condense titanium atoms than SPDN. This complexation allows for precipitation under lower pH conditions and accounts for the extended range of reaction.

The observed temperature effects may also be explained by this method of metal complexation. As the temperature increases, metal complexation, condensation, and initial nucleation also increase. Because most of the titanium is used for initial nucleation, less is left in solution for growth and smaller nanoparticles are formed at higher temperatures. As described above, SPN more easily complexes and condenses the titanium, which promotes faster precipitation. As a result, temperature does not dramatically affect particle size with SPN.

While the polyamines induce initial precipitation, the nanoparticles themselves also have some surface reactivity. When TiBALDH (10 μL of 1 M stock) is added to washed, freshly precipitated nanoparticles, a decrease in the concentration of titanium in solution over time is observed, with a rate constant similar to k_{2obs}. These results suggest that the nanoparticles themselves may promote the growth phase of the reaction.

Conclusion

Spermidine and spermine are biocatalysts for the precipitation of nanostructured titanium oxide in aqueous solution at room temperature. These reactions proceed in the absence of phosphate. Given that naturally occurring polyamines, including spermidine and spermine, are found in most cells, the observations reported here may explain the incorporation of titanium in diatom frustules and the prevalence of titanium in some invertebrate and even human cancer cells. This work helps to further elucidate the mechanisms of biotitanification.

Acknowledgment. We thank Dr. Christopher Incarvito for assistance with XRD, Dr. Zhenting Jiang for help with SEM, and Dr. Eric Paulson for help with NMR. We also thank Mr. Daryl Smith for help with annealing experiments and Mr. Marc Michel for assistance with the JCPDS-PDF database. K.E.C. was supported by a National Institutes of Health Predoctoral Traineeship in Biophysical Chemistry (GM08283). We also acknowledge the Yale University Department of Chemistry for support.

Supporting Information Available. Table of variable pH data, EDS spectra of bulk solids, histograms of particle size, XRD of solid precipitated from SPN, NMR spectra of solutions before and after reaction, SEM of variable-temperature SPDN experiments, SEM of variable-pH SPN experiments, and individual temperature plots for reactions with SPDN and SPN. This material is available free of charge via the Internet at http://pubs.acs.org.

References and Notes

(1) Cohen, S. S. *A Guide to the Polyamines*; Oxford University Press: New York, 1998.
(2) Wallace, H. M.; Fraser, A. V.; Hughes, A. *Biochem. J.* **2003**, *376*, 1−14.
(3) Jänne, J.; Alhonen, L.; Pietilä, M.; Keinänen, T. A. *Eur. J. Biochem.* **2004**, *271*, 877−894.
(4) Kröger, N.; Deutzmann, R.; Sumper, M. *Science* **1999**, *286*, 1129−1132.
(5) Kröger, N.; Deutzmann, R.; Bergsdorf, C.; Sumper, M. *Proc. Natl. Acad. Sci. U.S.A.* **2000**, *97*, 14133−14138.
(6) Sumper, M.; Brunner, E.; Lehmann, G. *FEBS Lett.* **2005**, *579*, 3765−3769.
(7) Kröger, N.; Lorenz, S.; Brunner, E.; Sumper, M. *Science* **2002**, *298*, 584−586.
(8) Sumper, M. *Angew. Chem., Int. Ed.* **2004**, *43*, 2251−2254.
(9) Sumper, M.; Kröger, N. *J. Mater. Chem.* **2004**, *14*, 2059−2065.
(10) Belton, D. J.; Patwardhan, S. V.; Perry, C. C. *J. Mater. Chem.* **2005**, *15*, 4629−4638.
(11) Belton, D.; Patwardhan, S. V.; Perry, C. C. *Chem. Commun.* **2005**, 3475−3477.
(12) Brunner, E.; Lutz, K.; Sumper, M. *Phys. Chem. Chem. Phys.* **2004**, *6*, 854−857.
(13) Lutz, K.; Gröger, C.; Sumper, M.; Brunner, E. *Phys. Chem. Chem. Phys.* **2005**, *7*, 2812−2815.
(14) Kröger, N.; Sumper, M. *Biomineralization*; Wiley−VCH: Weinheim, Germany, 2000.
(15) Xu, A. W.; Ma, Y. R.; Colfen, H. *J. Mater. Chem.* **2007**, *17*, 415−449.
(16) Orians, K. J.; Boyle, E. A.; Bruland, K. W. *Nature* **1990**, *348*, 322−325.
(17) Stokroos, I.; Litinetsky, L.; van der Want, J. J. L.; Ishay, J. S. *Nature* **2001**, *411*, 654−654.
(18) Ishay, J. S.; Riabinin, K.; Kozhevnikov, M.; van der Want, H.; Stokroos, I. *Biomacromolecules* **2003**, *4*, 649−656.
(19) Cole, K. E.; Valentine, A. M. *Dalton Trans.* **2006**, 430−432.
(20) Lavi, N.; Alfassi, Z. B. *Analyst* **1990**, *115*, 817−822.

(21) Carroll, K. G.; Tullis, J. L. *Nature* **1968**, *217*, 1172−1173.
(22) McCue, J. P. *Biochem. Med.* **1973**, *7*, 282−287.
(23) Barckhaus, R. H.; Schmidt, P. F. *Prog. Histochem. Cytochem.* **1991**, *23*, 332−341.
(24) Sholkovitz, E. R.; Price, N. B. *Geochim. Cosmochim. Acta* **1980**, *44*, 163−171.
(25) Martin, J. H.; Knauer, G. A. *Geochim. Cosmochim. Acta* **1973**, *37*, 1639−1653.
(26) Skrabal, S. A.; Ullman, W. J.; Luther, G. W. *Mar. Chem.* **1992**, *37*, 83−103.
(27) Riley, J. P.; Roth, I. *J. Mar. Biol. Assn. U.K.* **1971**, *51*, 63−72.
(28) Cole, K. E.; Ortiz, A. N.; Schoonen, M. A.; Valentine, A. M. *Chem. Mater.* **2006**, *18*, 4592−4599.
(29) Sewell, S. L.; Wright, D. W. *Chem. Mater.* **2006**, *18*, 3108−3113.
(30) Kroger, N.; Dickerson, M. B.; Ahmad, G.; Cai, Y.; Haluska, M. S.; Sandhage, K. H.; Poulsen, N.; Sheppard, V. C. *Angew. Chem., Int. Ed.* **2006**, *45*, 7239−7243.
(31) Yoe, J. H.; Armstrong, A. R. *Anal. Chem.* **1947**, *19*, 100−102.
(32) Eyring, H. *J. Chem. Phys.* **1935**, *3*, 107−115.
(33) Connors, K. A. *Chemical Kinetics*; VCH Publishers, Inc.: New York, 1990.
(34) Annenkov, V. V.; Patwardhan, S. V.; Belton, D.; Danilovtseva, E. N.; Perry, C. C. *Chem. Commun.* **2006**, 1521−1523.
(35) Naik, R. R.; Whitlock, P. W.; Rodriguez, F.; Brott, L. L.; Glawe, D. D.; Clarson, S. J.; Stone, M. O. *Chem. Commun.* **2003**, 238−239.
(36) Luckarift, H. R.; Spain, J. C.; Naik, R. R.; Stone, M. O. *Nat. Biotechnol.* **2004**, *22*, 211−213.
(37) Naik, R. R.; Tomczak, M. M.; Luckarift, H. R.; Spain, J. C.; Stone, M. O. *Chem. Commun.* **2004**, 1684−1685.
(38) Comba, P.; Merbach, A. *Inorg. Chem.* **1987**, *26*, 1315−1323.

BM061221L